

Competitive ArC–H and ArC–X (X = Cl, Br) Activation in Halobenzenes at Cationic Titanium Centers

Kuangbiao Ma, Warren E. Piers,* and Masood Parvez

Contribution from the Department of Chemistry, University of Calgary,
2500 University Drive N.W., Calgary, Alberta, Canada T2N 1N4

Received December 9, 2005; E-mail: wpiers@ucalgary.ca

Abstract: The titanium methyl cation $[\text{Cp}^*(\text{Bu}_3\text{P}=\text{N})\text{TiCH}_3]^+[\text{B}(\text{C}_6\text{F}_5)_4]^-$ reacts rapidly with H_2 to give the analogous cationic hydride $[\text{Cp}^*(\text{Bu}_3\text{P}=\text{N})\text{TiH}(\text{THF})_n]^+[\text{B}(\text{C}_6\text{F}_5)_4]^-$ ($n = 0, 1$), which can be trapped and isolated as its THF adduct $\mathbf{1}\cdot\text{THF}$ ($n = 1$). When generated in the presence of chloro or bromobenzene, $\mathbf{1}$ undergoes C–X activation or *ortho*-C–H activation, depending on the amount of dihydrogen present in the reaction medium. At ~ 4 atm of H_2 , C–X activation is preferred, giving the halocations $[\text{Cp}^*(\text{Bu}_3\text{P}=\text{N})\text{TiX}]^+[\text{B}(\text{C}_6\text{F}_5)_4]^-$ ($\mathbf{2X}$) and C_6H_6 /biphenyl mixtures. At lower pressures of H_2 (> 1 atm), the β -halophenyl cations $[\text{Cp}^*(\text{Bu}_3\text{P}=\text{N})\text{Ti}(2\text{-X-C}_6\text{H}_4)]^+[\text{B}(\text{C}_6\text{F}_5)_4]^-$ ($\mathbf{3X}$) are the products isolated. In the absence of H_2 , these compounds are quite thermally stable, but undergo β -halogen elimination upon moderate heating, to give $\mathbf{2X}$ ($\sim 20\%$) and compounds $\mathbf{4X}$ which are the result of reaction between $\mathbf{2X}$ and benzyne via addition of the benzyne C–C triple bond across the Ti–N bond of the phosphinimide ligand. Thus, three separate bond activation processes are operative in this system: direct C–X activation, *ortho*-C–H activation, and indirect C–X activation via β -halogen elimination. Mechanistic studies on all three processes have been done and support a radical pathway for direct C–X cleavage, σ -bond metathesis of the *ortho*-C–H bond of η^1 -coordinated $\text{C}_6\text{H}_5\text{X}$, and β -halogen elimination from base-free compound $\mathbf{3X}$.

Introduction

The selective activation of aryl halide bonds is a key step in dozens of transition metal catalyzed coupling protocols or ArX bond activations.¹ Despite its importance, the intimate mechanism of the $\text{C}_{\text{aryl}}\text{--X}$ cleavage step is not generally known in detail² and may involve concerted oxidative addition, nucleophilic aromatic substitution ($\text{S}_{\text{N}}\text{Ar}2$), or some mechanism involving radicals. In addition, competitive processes involving the activation of the $\text{C}_{\text{aryl}}\text{--H}$ bonds present in these substrates can further complicate the chemistry involved in the reactions of aryl halides with transition metal complexes.³ A better understanding of the interplay between these various pathways will lead to more selective and active catalysts for transformation of these plentiful substrates.

Although catalytic protocols involving late metal based catalyst systems are more widely practiced,¹ it has been known for some time that d^0 early transition metal compounds are

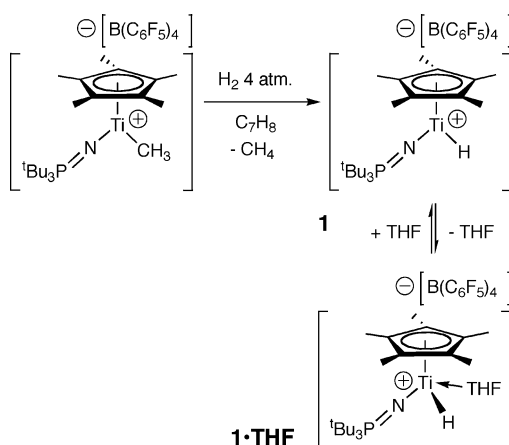
highly reactive toward aryl halides, particularly those with metal hydride functions. For example, both neutral⁴ and cationic⁵ zirconocene hydrides have been observed to react with fluoro- and chloroaromatic substrates. Lanthanocene hydrides, isoelectronic to the cationic group 4 metallocenium ions, also react with aryl halides to give often ill-defined mixtures of products,⁶ stemming at least in part from β -halo elimination processes involving the kinetic products of *ortho*-C–H bond activation via σ -bond metathesis.⁷ This nonredox pathway is generally thought to be dominant, although observations that the thermodynamic products where the halogen atom is transferred to the electrophilic metal are sometimes assisted by light⁵ indicating that one-electron redox processes may be involved for those metals that can access lower oxidation states.⁸

Monomeric d^0 metal hydrides, because of their high reactivity, are generally rare and difficult to study and often must be generated in situ via hydrogenolysis or dissociation from dimeric or oligomeric⁹ structures. Thus, harnessing their potential for

- (1) (a) *Metal Catalyzed Cross-Coupling Reactions*, 2nd ed.; de Mijere, A., Diederich, F., Eds.; Wiley-VCH: Weinheim, Germany, 2004. (b) Negishi, E. I., Ed. *Handbook of Organopalladium Chemistry for Organic Synthesis*; Wiley-Interscience: New York, 2002.
- (2) Recent mechanistic studies on Ar–X activation: (a) Barrios-Landeros, F.; Hartwig, J. F. *J. Am. Chem. Soc.* **2005**, *127*, 6944. (b) Littke, A. F.; Fu, G. C. *Angew. Chem., Int. Ed.* **2002**, *41*, 4176. (c) Lewis, A. K. de K.; Caddick, S.; Cloke, F. G. N.; Billingham, N. C.; Hitchcock, P. B.; Leonard, J. J. *Am. Chem. Soc.* **2003**, *125*, 10066. (d) Espinet, P.; Echavarren, A. M. *Angew. Chem., Int. Ed.* **2004**, *43*, 4704. (e) Galardon, E.; Ramdeehul, S.; Brown, J. M.; Cowley, A.; Hii, K. K.; Jutand, A. *Angew. Chem., Int. Ed.* **2002**, *41*, 1760.
- (3) Recent examples employing late metals: (a) Fan, L.; Parkin, S.; Ozerov, O. V. *J. Am. Chem. Soc.* **2005**, *127*, 16772. (b) Ben-Ari, E.; Gandelman, M.; Rozenberg, H.; Shimon, L. J. W.; Milstein, D. *J. Am. Chem. Soc.* **2003**, *125*, 4714. (c) Zhang, X.; Kanzelberger, M.; Emge, T. J.; Goldman, A. S. *J. Am. Chem. Soc.* **2004**, *126*, 13192.

- (4) (a) Jones, W. D. *Dalton Trans.* **2003**, 3991 and references therein. (b) Turculet, L.; Tilley, T. D. *Organometallics* **2002**, *21*, 3961. (c) Kraft, B. M.; Jones, W. D. *J. Am. Chem. Soc.* **2002**, *124*, 8681. (d) Clot, E.; Megret, C.; Kraft, B. M.; Eisenstein, O.; Jones, W. D. *J. Am. Chem. Soc.* **2004**, *126*, 5647.
- (5) Wu, F.; Dash, A.; Jordan, R. F. *J. Am. Chem. Soc.* **2004**, *126*, 15360.
- (6) Booiij, M.; Deelman, B.-J.; Duchateau, R.; Postma, D. S.; Meetsma, A.; Teuben, J. H. *Organometallics* **1993**, *12*, 3531.
- (7) Maron, L.; Werkema, E. L.; Perrin, L.; Eisenstein, O.; Andersen, R. A. *J. Am. Chem. Soc.* **2005**, *127*, 279.
- (8) Other recent examples of ArX reactions with d^0 metal hydrides: (a) Gavenonis, J.; Tilley, T. D. *Organometallics* **2004**, *23*, 31. (b) Deutsch, P. P.; Maguire, J. A.; Jones, W. D.; Eisenberg, R. *Inorg. Chem.* **1990**, *29*, 686.
- (9) (a) Ephritikhine, M. *Chem. Rev.* **1997**, *97*, 2193. (b) Emslie, D. J.; Piers, W. E. *Coord. Chem. Rev.* **2002**, *233–34*, 129.

Scheme 1



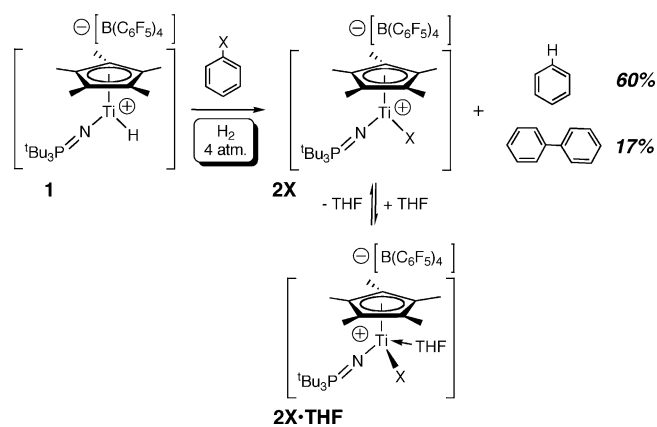
mediating useful chemical transformations has been hampered by the difficulties in performing detailed mechanistic studies utilizing well-defined hydride complexes. Recently, we prepared and fully characterized a reasonably stable half metallocene titanium(IV) hydrido species, $[\text{Cp}^*(\text{Bu}_3\text{P}=\text{N})\text{TiH}(\text{THF})_n]^+[\text{B}(\text{C}_6\text{F}_5)_4]^-$ ($n = 0$, **1**; $n = 1$, **1·THF**),¹⁰ stabilized by a bulky phosphinimide donor.¹¹ While this material can be very cleanly generated in solution or isolated as a THF adduct, it undergoes a number of facile bond activation reactions, including ones involving chloro- and bromobenzene. Here we describe in detail the chemistry involved in these reactions and expose the operation of diverse mechanisms of C–X and C–H bond activations depending on the conditions employed.

Results and Discussion

Synthetic Studies. As previously reported, the cationic methyl complex $[\text{Cp}^*(\text{Bu}_3\text{P}=\text{N})\text{TiCH}_3]^+[\text{B}(\text{C}_6\text{F}_5)_4]^-$ can be cleanly generated in toluene, bromobenzene, or chlorobenzene by activation of the neutral dimethyl precursor with $[\text{Ph}_3\text{C}]^+[\text{B}(\text{C}_6\text{F}_5)_4]^-$.¹² In nonhalogenated solvents, such as toluene, this species reacts rapidly with H_2 to give a monomeric cationic titanium hydride complex, **1**, which can be trapped as its THF adduct, **1·THF**, and fully characterized by NMR spectroscopy and X-ray crystallography. This chemistry is summarized in Scheme 1. Solutions of base-free **1** are stable in the presence of an excess of H_2 for at least several hours, but upon removal of the dihydrogen atmosphere, **1** decomposes to a mixture of products, some derived from reaction with the toluene solvent,¹³ and thus is not isolable as a base-free titanium hydrido complex.

In the presence of haloarenes, however, hydride **1** effects bond activation of either the C–X or the *ortho*-C–H bonds via two competing processes that are partitioned by the amount of dihydrogen present in the system. For example, hydrogenolysis of $[\text{Cp}^*(\text{Bu}_3\text{P}=\text{N})\text{TiCH}_3]^+[\text{B}(\text{C}_6\text{F}_5)_4]^-$ using 4 atm of H_2 in

Scheme 2



chloro- or bromobenzene solvent resulted in quantitative production of the titanium halocations $[\text{Cp}^*(\text{Bu}_3\text{P}=\text{N})\text{TiX}]^+[\text{B}(\text{C}_6\text{F}_5)_4]^-$ ($\text{X} = \text{Cl}$, **2Cl**; $\text{X} = \text{Br}$, **2Br**) as the titanium-containing products (Scheme 2). In the reaction involving $\text{C}_6\text{H}_5\text{Br}$, formation of **2Br** is accompanied by generation of benzene and biphenyl¹⁴ in the ratios shown in the scheme, accounting for a total of ~ 1 equiv of bromobenzene used in the reaction. The identity of the organic byproducts was verified by ^1H NMR spectroscopy and GCMS analysis; when the reaction is carried out using D_2 , benzene- d_1 is produced. These reactions are facile at room temperature when vigorously stirred (reaction complete in ~ 5 min) and occur equally well in the absence of light, with no significant change in the benzene:biphenyl ratio.

The halocations **2X** are isolable as solids and appear to be monomeric, although this has not been conclusively demonstrated. ESI-MS analysis of **2Br** showed that the water adduct was the major species ($M^+ = 497$), but a minor peak at $M^+ = 479$ has an isotope pattern consistent with a monomeric structure for **2Br**. A C_5H_5 -supported analogue of **2Cl** has been shown to be dimeric with *trans* disposed phosphinimide ligands across the Ti_2Cl_2 core.¹⁵ However, the sterically more bulky Cp^* ligands employed here, in conjunction with the electrostatic destabilization inherent in a dicationic dimer, may be enough to render compounds **2X** monomeric. Furthermore, there is no evidence for *rac/meso* diastereomers, which might be expected in dimers with more equisteric ligands (Cp^* and $\text{Bu}_3\text{P}=\text{N}$).¹⁶ In any case, both of these compounds readily form monomeric THF adducts **2X·THF** when treated with THF. The identities of **2Cl** and **2Cl·THF** were also confirmed by their independent syntheses via treatment of $\text{Cp}^*(\text{Bu}_3\text{P}=\text{N})\text{Ti}(\text{Cl})\text{CH}_3$ with $[\text{Ph}_3\text{C}]^+[\text{B}(\text{C}_6\text{F}_5)_4]^-$, cleanly generating solutions of **2Cl** that were spectroscopically identical to those obtained by reaction of **1** with $\text{C}_6\text{H}_5\text{Cl}$. Furthermore, the X-ray structure of **2Br·THF** was obtained, and a Crystallmaker depiction of the cationic portion of this molecule is shown in Figure 1, along with

(10) Ma, K.; Piers, W. E.; Gao, Y.; Parvez, M. *J. Am. Chem. Soc.* **2004**, *126*, 5668.

(11) Stephan, D. W. *Organometallics* **2005**, *24*, 2548 and references therein.

(12) Chien, J. C. W.; Tsai, W.-M.; Rausch, M. D. *J. Am. Chem. Soc.* **1991**, *113*, 8570.

(13) (a) The major product observed is the benzyl cation $[\text{Cp}^*(\text{Bu}_3\text{P}=\text{N})\text{TiCH}_2\text{Ph}]^+[\text{B}(\text{C}_6\text{F}_5)_4]^-$, which can be trapped as its THF adduct $[\text{Cp}^*(\text{Bu}_3\text{P}=\text{N})\text{TiCH}_2\text{Ph}(\text{THF})]^+[\text{B}(\text{C}_6\text{F}_5)_4]^-$. The identity of this compound was confirmed by separate synthesis. The mechanism of its formation is unknown, but the preference for the benzyl species is not consistent with a σ -bond metathesis mechanism^{13b} unless this is the thermodynamic isomer in this system. (b) Thompson, M. E.; Baxter, S. M.; Bulls, A. R.; Burger, B. J.; Nolan, M. C.; Santarsiero, B. D.; Schaefer, W. P.; Bercaw, J. E. *J. Am. Chem. Soc.* **1987**, *109*, 203.

(14) Small amounts of what we presume to be cyclohexylbenzene ($\sim 3\%$) and trace quantities ($< 1\%$) of bromobiphenyl were also observed in the $\text{C}_6\text{H}_5\text{Br}$ reaction. The observation of small amounts of partially hydrogenated biphenyl is curious and under further investigation. The GCMS data do not allow us to conclusively identify the product as cyclohexylbenzene, but it is clear from the use of $\text{D}_2/\text{C}_6\text{H}_5\text{X}$ or $\text{H}_2/\text{C}_6\text{D}_5\text{X}$ that six hydrogen or deuterium atoms are incorporated. Cationic hydride **1** has also been observed to rapidly hydrogenate anthracene to tetrahydroanthracene (Ma, K.; Piers, W. E. Unpublished results).

(15) (a) Cabrera, L.; Hollink, E.; Stewart, J. C.; Wei, P.; Stephan, D. W. *Organometallics* **2005**, *24*, 1091. (b) Yue, N. L. S.; Stephan, D. W. *Organometallics* **2001**, *20*, 2303.

(16) See for example: Zhang, S.; Piers, W. E. *Organometallics* **2001**, *20*, 2088.

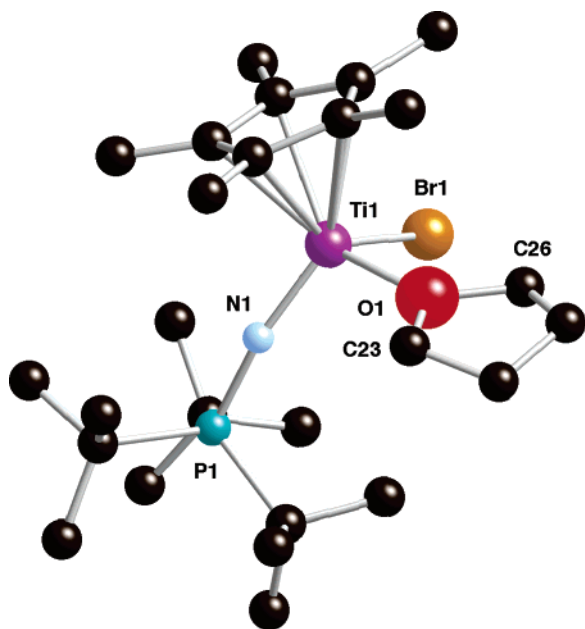


Figure 1. Crystalmaker depiction of the molecular structure of the cation in **2Br·THF** (hydrogens omitted for clarity). Selected bond distances (Å): Ti(1)–Br(1), 2.4365(12); Ti(1)–N(1), 1.780(5); Ti(1)–O(1), 2.084(4); P(1)–N(1), 1.629(5). Selected bond angles (°): N(1)–Ti(1)–O(1), 103.1(2); N(1)–Ti(1)–Br(1), 104.4(2); O(1)–Ti(1)–Br(1), 93.8(2); Ti(1)–N(1)–P(1), 165.7(3); C(23)–O(1)–Ti(1), 125.1(3); C(26)–O(1)–Ti(1), 125.6(3).

selected metrical data.¹⁷ The Ti center has a three-legged piano stool geometry with no close contacts to the borate anion. The Ti(1)–N(1) distance, which does not vary much in a range of titanium phosphinimido compounds,¹¹ is typical at 1.780(5) Å. However, distances from Ti(1) to the O(1) and Br(1) atoms are shorter than most comparable literature bond lengths, due to the cationic charge of the complex and its low formal coordination number. For example, the Ti(1)–Br(1) distance in **2Br·THF** is ~0.1 Å shorter than the distances in a neutral titanocene dibromide,¹⁸ and the Ti(1)–O(1) length of 2.084(4) Å is shorter than that observed in $[\text{Cp}^*_2\text{TiCH}_3(\text{THF})]^+[\text{BPh}_4]^-$ (2.154(6) Å).¹⁹

When **1** is generated in $\text{C}_6\text{D}_5\text{X}$ under 4 atm of H_2 and the reaction monitored by ^1H NMR spectroscopy (Figure 2, illustrated for X = Br), two important observations are made. First, essentially complete conversion to **2Br** is accomplished in less than 6 min under these conditions. Second, another prominent species is observed to form early in the reaction, which eventually gets converted to the bromotitanium cation product. This species can be generated quantitatively (by NMR spectroscopy) and isolated in good yields by carrying out the reaction at pressures of less than 1 atm of dihydrogen. In fact, use catalytic amounts of dihydrogen or the titanium hydride **1** converts $[\text{Cp}^*(\text{Bu}_3\text{P}=\text{N})\text{TiCH}_3]^+[\text{B}(\text{C}_6\text{F}_5)_4]^-$ into these products, which were identified as the *ortho*-halophenyl cations $[\text{Cp}^*(\text{Bu}_3\text{P}=\text{N})\text{Ti}(2\text{-X-C}_6\text{H}_4)]^+[\text{B}(\text{C}_6\text{F}_5)_4]^-$ (X = Cl, **3Cl**; X = Br, **3Br**) by NMR spectroscopy and the solid-state characterization of their THF adducts **3X·THF** (Scheme 3). The β -haloaryl cations **3X** exhibit the expected ligand resonances

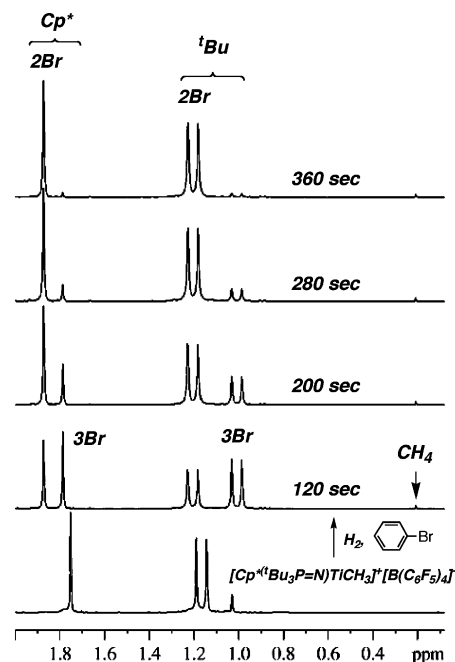
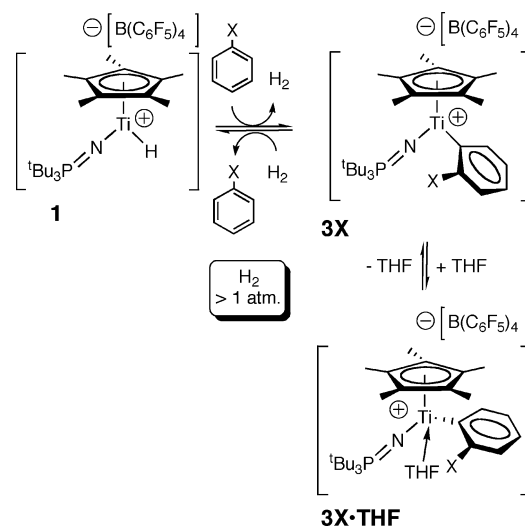


Figure 2. Partial ^1H NMR spectra of the preceding reaction between $[\text{Cp}^*(\text{Bu}_3\text{P}=\text{N})\text{TiCH}_3]^+[\text{B}(\text{C}_6\text{F}_5)_4]^-$ (bottom spectrum) and H_2 (4 atm) in bromobenzene- d_5 at room temperature. The spectra show the initial appearance of signals for **3Br**, formed competitively with **2Br**, and eventual complete conversion to **3Br**.

Scheme 3



in the ^1H and ^{31}P NMR spectra, as well as four characteristic resonances in the ^1H NMR spectra for the remaining C–H aromatic protons. When solutions of **3X** are exposed to 4 atm of H_2 at room temperature, conversion to the halide cations **2X** is observed, presumably via regenerated **1** and ArX .

The X-ray structures of **3Cl·THF** and **3Br·THF** were both obtained, and the molecular structures are shown in Figures 3 and 4, respectively. The two compounds are isostructural and exhibit three-legged piano stool (tetrahedral) geometry about the titanium center; both crystallize with a second, noncoordinated THF molecule in the crystal lattice, which is apparent also from the elemental analysis data (see Experimental Section). Ti(1)–N(1) and Ti(1)–O(1) distances are slightly elongated in comparison to those in **2Br·THF**, reflecting greater steric congestion about the metal in compounds **3X·THF**. Most

(17) Full details on this particular structure can be found in the Supporting Information of ref 10.

(18) Klouras, N.; Nastopoulos, V.; Demekopoulos, I.; Leban, I. *Z. Anorg. Allg. Chem.* **1993**, *619*, 1927.

(19) Bochmann, M.; Jaggar, A. J.; Wilson, L. M.; Hursthouse, M. B.; Motevalli, M. *Polyhedron* **1989**, *8*, 1838.

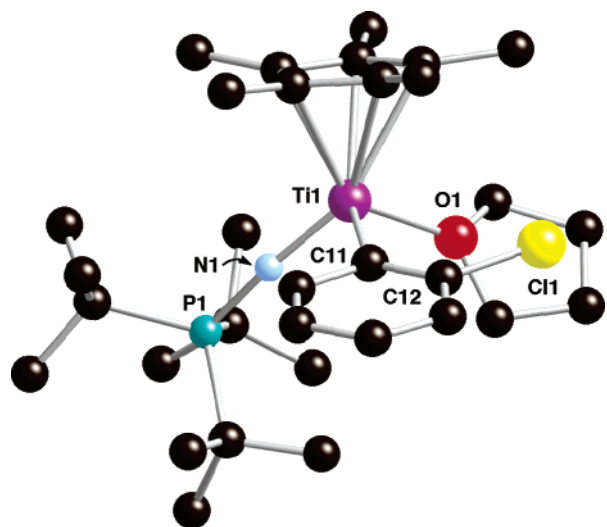


Figure 3. Crystallmaker depiction of the molecular structure of the cation in **3Cl·THF** (hydrogens and the THF of crystallization omitted for clarity). Selected bond distances (Å): Ti(1)–C(11), 2.170(3); Ti(1)–N(1), 1.791(2); Ti(1)–O(1), 2.103(2); P(1)–N(1), 1.616(2); C(12)–Cl(1), 1.767(4). Selected nonbonded distance (Å): Ti(1)⋯Cl(1), 3.657. Selected bond angles (°): N(1)–Ti(1)–O(1), 101.96(10); N(1)–Ti(1)–C(11), 98.82(12); O(1)–Ti(1)–C(11), 103.15(11); Ti(1)–N(1)–P(1), 171.65(16); Ti(1)–C(11)–C(12), 129.7(3); C(11)–C(12)–Cl(1), 120.3(3).

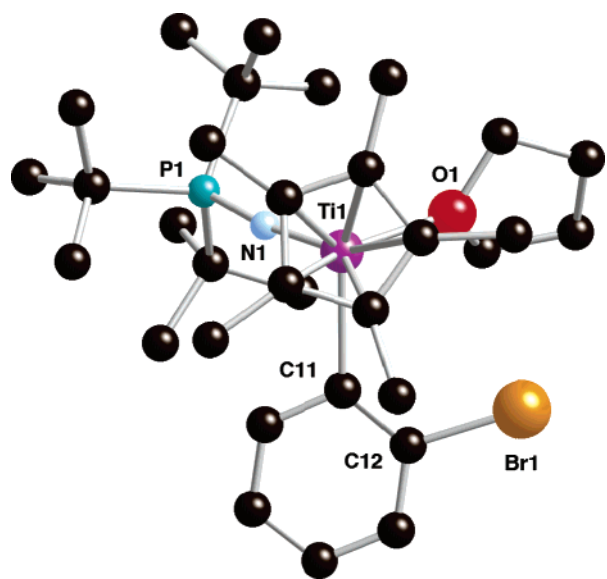


Figure 4. Crystallmaker depiction of the molecular structure of the cation in **3Br·THF** (hydrogens and the THF of crystallization omitted for clarity). Selected bond distances (Å): Ti(1)–C(11), 2.274(14); Ti(1)–N(1), 1.787(15); Ti(1)–O(1), 2.113(12); P(1)–N(1), 1.619(4); C(12)–Br(1), 1.931(6). Selected nonbonded distance (Å): Ti(1)⋯Br(1), 3.841. Selected bond angles (°): N(1)–Ti(1)–O(1), 101.4(6); N(1)–Ti(1)–C(11), 95.8(7); O(1)–Ti(1)–C(11), 101.1(6); Ti(1)–N(1)–P(1), 171.1(4); Ti(1)–C(11)–C(12), 129.8(5); C(11)–C(12)–Cl(1), 121.6(4).

notably, there does not appear to be any interaction between the titanium center and the β -halogens as indicated by the long Ti(1)–X(1) distances (3.657 Å, X = Cl; 3.841 Å, X = Br), and in contrast to observations for a related $[\text{Cp}^*\text{Zr}(\eta^2\text{-C}_6\text{H}_4\text{-2-Cl-C}_6\text{H}_4)(\text{CH}_3\text{CN})]^+[\text{B}(\text{C}_6\text{F}_5)_4]^-$ reported by Jordan et al. in which there is a β -chloro metal interaction, 2.831(1) Å.⁵ Furthermore, the C(11)–C(12)–X(1) angles are close to 120°, and the Ti(1)–C(11)–C(12) angles are \sim 129°; both of these angles (particularly the latter) would be expected to contract in the event of significant metal– β -halo interaction. While such

Table 1. Summary of Data Collection and Structure Refinement Details for **3Cl·THF**, **3Br·THF**, and **4Cl**

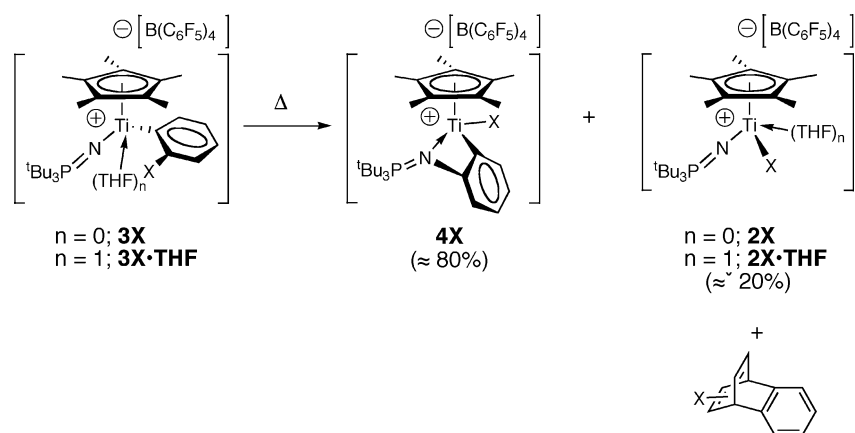
	3Cl·THF	3Br·THF	4Cl
formula	$\text{C}_{60}\text{H}_{62}\text{BClF}_{20}\text{-NO}_2\text{PTi}$	$\text{C}_{60}\text{H}_{62}\text{BBrF}_{20}\text{-NO}_2\text{PTi}$	$\text{C}_{52}\text{H}_{46}\text{BClF}_{20}\text{-NPTi}$
fw	1334.24	1378.70	1190.03
temp, K	173(2)	173(2)	173(2)
cryst syst	triclinic	triclinic	triclinic
space group	$P\bar{1}$	$P\bar{1}$	$P\bar{1}$
<i>a</i> , Å	12.165(2)	12.244(2)	12.343(2)
<i>b</i> , Å	14.823(3)	14.765(6)	14.797(3)
<i>c</i> , Å	17.749(3)	17.718(4)	14.932(4)
α , deg	71.616(15)	71.772(7)	83.933(9)
β , deg	77.542(12)	77.525(6)	89.154(9)
γ , deg	84.788(8)	84.712(7)	67.536(15)
<i>V</i> , Å ³	2964.8(9)	2969.5(8)	2505.0(9)
<i>Z</i>	2	2	2
<i>d</i> _{calcd} , mg m ^{−3}	1.495	1.542	1.578
μ , mm ^{−1}	0.324	0.951	0.370
cryst size, mm	0.16 × 0.12 × 0.08	0.14 × 0.13 × 0.06	0.20 × 0.10 × 0.06
no. of rflns measd	25213	25258	16510
no. of unique rflns	13325	13405	8781
<i>R</i> ₁ / <i>wR</i> ₂	0.058/0.134	0.076/0.206	0.0417/0.1003
gof	0.996	0.97	0.999
res density, e/Å ³	0.55/−0.51	1.53/−1.66	0.282/−0.506

an interaction may be at play in the base-free compounds **3X**, it appears that ligation of the THF easily displaces this weaker intramolecular dative bond. While it might be reasonable to suggest that these β -haloaryl cations are *intermediates* along the way to the thermodynamic products **2X** via the process described above in Scheme 2, several lines of evidence suggest that this is not the case. In the absence of H₂, products **3X** are relatively stable species at ambient temperature, but convert to the thermodynamically favored halocations **2X** at a rate that (qualitatively) depends on the amount of hydrogen present. In the complete absence of H₂, compounds **3X** (and **3X·THF**) do undergo conversion to the halocations **2X**, but at a much slower rate than observed in the presence of H₂. Furthermore, **2X** cations are the *minor* products in this reaction, the major species being the benzyne adducts **4X**, strongly implicating a β -halogen elimination pathway (Scheme 4) for this chemistry. Adducts **4X** comprise \sim 80% of the product mixture, while compounds **2X** form in roughly 20% yield. Formation of **2Cl** or **2Br** is accompanied by various side products arising from the reaction of “C₆H₄”, benzyne, with the haloarene solvent employed (primarily regioisomeric Diels–Alder adducts). These products were identified by GCMS in the reaction mixture, which also included trace amounts of a product arising from benzyne/Cp* coupling.

The major products of β -halogen elimination, **4X**, were identified by their NMR spectra, and the structure was confirmed by X-ray crystallography on suitable crystals of **4Cl**; the molecular structure is shown in Figure 5. To produce compounds **4**, the benzyne that is eliminated upon β -X elimination is trapped by the Ti–N bond in **2X**, forming a new Ti–C_{aryl} bond and converting the phosphinimido ligand into a neutral phosphinimine ligand. This is indicated by the significant lengthening of the Ti(1)–N(1) bond to 2.051(2) Å²⁰ and the bending of the Ti(1)–N(1)–P(1) angle from \sim 170 to 139.45(14)°. The ³¹P

(20) A similar lengthening in the complex $[(\text{Ph}_3\text{P}=\text{N})(\text{Ph}_3\text{P}=\text{NH})\text{TiF}_3]_2$, which contains both phosphinimido (Ti–N = 1.777(4) Å) and phosphinimine (Ti–N = 2.134(4) Å) ligands, was observed: Grun, M.; Harms, K.; zu Kocker, R. M.; Dehnicke, K.; Goesmann, H. *Z. Anorg. Allg. Chem.* **1996**, 622, 1091.

Scheme 4



NMR chemical shifts for the phosphinimine ligands of compounds **4** appear at ~ 81 ppm, shifted downfield by approximately 24–25 ppm in comparison to the anionic ligands. The angles within the Ti(1)–C(12)–N(1) ring are as expected, and the angle between the planes defined by C(12)–C(11)–N(1) and C(12)–Ti(1)–N(1) is $20.8(2)^\circ$, indicating a slightly puckered ring; the Ti(1)–C(11) distance is $2.421(3)$ Å.

Mechanistic Considerations and Studies. The above observations suggest that compounds **3X** are kinetic products of the reaction of cationic hydride **1** with $\text{C}_6\text{H}_5\text{X}$ that are *not* intermediates on the low energy pathway to the thermodynamic products **2X** observed in the presence of H_2 . Thus, three mechanistically distinct bond activation processes are operational in the chemistry involving cationic hydride **1** with chloro- and bromobenzene: direct C–X bond activation, *ortho*-C–H bond activation, and β -halo elimination from compounds **3**. To test this hypothesis and probe the mechanisms of the various processes involved, further studies were performed as described in the following sections.

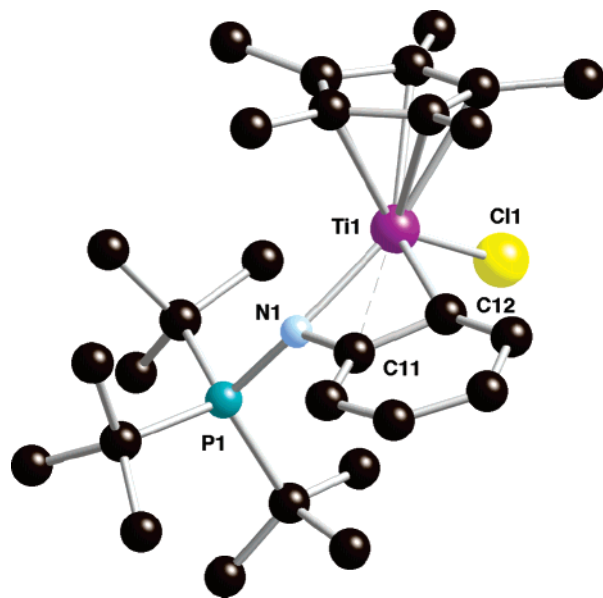
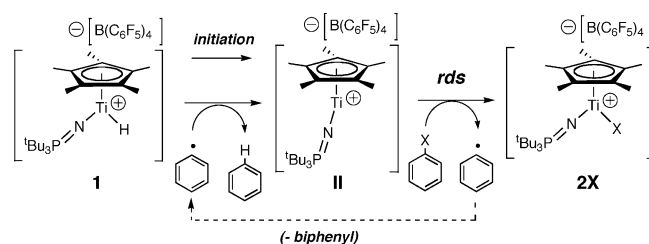
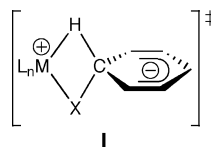


Figure 5. Crystallographic depiction of the molecular structure of the cation in **4Cl** (hydrogens omitted for clarity). Selected bond distances (Å): Ti(1)–Cl(1), 2.2642(10); Ti(1)–C(12), 2.037(3); Ti(1)–N(1), 2.051(2); P(1)–N(1), 1.644(2). Selected nonbonded distance (Å): Ti(1)–C(11), 2.421(3). Selected bond angles ($^\circ$): N(1)–Ti(1)–Cl(1), $116.15(7)$; N(1)–Ti(1)–C(12), $71.51(10)$; Cl(1)–Ti(1)–C(12), $99.76(9)$; Ti(1)–N(1)–P(1), $139.45(14)$; Ti(1)–C(12)–C(11), $57.18(15)$; Ti(1)–N(1)–C(11), $85.31(14)$; C(12)–C(11)–N(1), $112.5(2)$.

Scheme 5



Direct Activation of ArX. Proposed pathways for the direct reaction of ArX with M–H to give M–X and ArH include σ -bond metathesis-like transition states (**I**) or stepwise pathways that invoke nucleophilic attack on the aryl halide followed by β -halo transfer to the metal. The latter path is likely for systems where the metal hydride is hydridic in character (e.g., $\text{Cp}^*_{-2}\text{-ZrH}_2$) and the aryl halide is highly electrophilic, for example, C_6F_6 .²¹ This is not a high probability scenario where **1** and $\text{C}_6\text{H}_5\text{-Cl}$ or $\text{C}_6\text{H}_5\text{-Br}$ are concerned. Furthermore, σ -bond metathesis transition states, such as **I**, are computed to be rather high in energy⁷ due to the positioning of carbon in the β -position of the kite-shaped transition state and thus are also improbable for such a transformation.



Given the biphenyl product observed (Scheme 2) in this reaction, it appears most likely that conversion of **1** to **2X** is mediated by trace amounts of Ti(III) species generated from **1** in the presence of H_2 (Scheme 5). Previously, we have observed that the putative C_5H_5 (Cp) analogue of **1**, generated by treatment of $[\text{Cp}(\text{tBu}_3\text{P}=\text{N})\text{TiCH}_3]^+[\text{B}(\text{C}_6\text{F}_5)_4]^-$ with H_2 , is rapidly reduced to “ $[\text{Cp}(\text{tBu}_3\text{P}=\text{N})\text{Ti}]^+[\text{B}(\text{C}_6\text{F}_5)_4]^-$ ” presumably by homolysis of the Ti–H bond.¹⁰ Although the more donating and sterically protecting Cp^* ligand stabilizes the Ti(IV) hydride **1**, it is conceivable that the Ti(III) cation shown in the scheme is generated in enough quantities to initiate the cycle shown. Once generated, abstraction of X• from ArX by the Ti(III) cation **II**²² (Scheme 5) yields the products **2X** and a phenyl radical. This is likely the rate-limiting step since, in a competition

(21) Kraft, B. M.; Jones, W. D. *J. Organomet. Chem.* **2002**, 658, 132.

experiment in which **1** is generated in the presence of a mixture of C_6H_5Cl/C_6F_5Br , **2Br** is formed preferentially (**2Br**:**2Cl** \approx 27:1) as would be expected given the weaker C–Br versus C–Cl bond.^{23,24} The phenyl radicals produced rapidly abstract a hydrogen atom from **1**, regenerating $[Cp^*(tBu_3P=N)Ti^{III}]^+ [B(C_6F_5)_4]^-$; as the concentration of **1** is depleted, phenyl radicals dimerize, yielding biphenyl.²⁵ High concentrations of H_2 are necessary to convert the kinetically favored compounds **3X** back to **1**, effectively maintaining high concentrations of the hydride, the source of Ti(III).

The above scenario is supported by a series of experiments wherein the hydrogenolysis of $[Cp^*(tBu_3P=N)TiCH_3]^+ [B(C_6F_5)_4]^-$ in chlorobenzene is monitored by ESR spectroscopy. While solutions of neutral starting material $Cp^*(tBu_3P=N)TiCH_3_2$ are ESR silent, upon activation with $[Ph_3C]^+ [B(C_6F_5)_4]^-$, detectable amounts of trityl radical are present, as shown in Figure 6a,²⁶ suggesting that the trityl reagent activates the titanium dimethyl by both abstractive²⁷ and oxidative²⁸ pathways. While no titanium(III) species are observed in these solutions, upon hydrogenolysis, evidence for the trityl radical disappears and a strong signal (295 K, $g = 1.984$ G, Figure 6b) assignable to a titanium-centered paramagnet emerges in the spectrum and grows in intensity as the reaction proceeds. The line width of the signal is reasonably narrow (~ 5 G), but no discernible hyperfine coupling is observed either to the ligand nuclei or titanium isotopes (^{47}Ti , $I = 5/2$, 7.28%; ^{49}Ti , $I = 7/2$, 5.51%). The lack of hyperfine coupling is common in related metallocene Ti(III) complexes, although in some cases, coupling to the spin-active Ti isotopes is discernible.²⁹ Nonetheless, given that the g value is similar to others reported in the literature,²⁹ these experiments provide strong evidence that a Ti(III) species is generated under these conditions. It is likely, therefore, that the small quantities of trityl radical present in these solutions³⁰ initiate the direct C–X bond activation chemistry; upon close

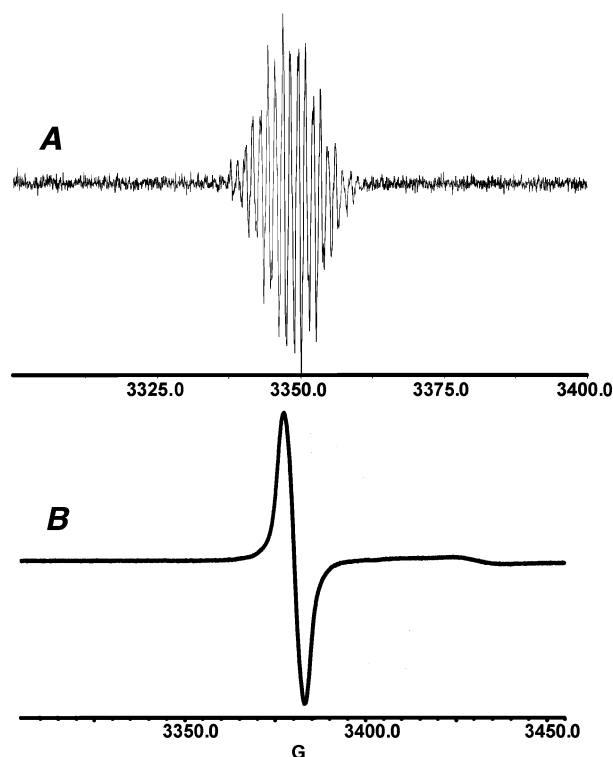


Figure 6. ESR spectra (295 K) of (a) $Ph_3C\cdot$ formed during the in situ generation of $[Cp^*(tBu_3P=N)TiCH_3][B(C_6F_5)_4]$ in chlorobenzene ($g = 2.003$). (b) Tube \approx 40 min after H_2 (4 atm) was admitted to the sample. The intense signal ($g = 1.984$) is assigned to a Ti(III) species generated upon H_2 generation.

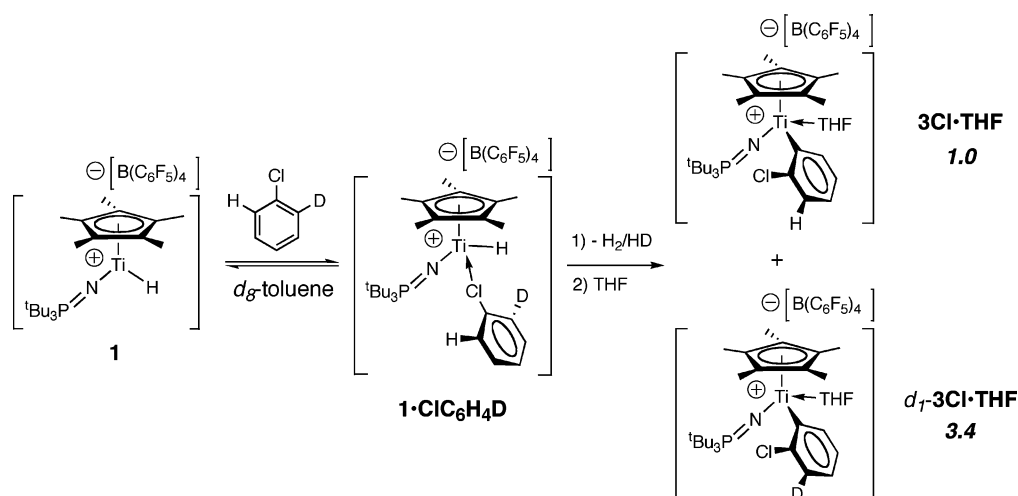
examination of the GCMS traces of these reactions, small amounts of Ph_3CH are indeed observed. Once conversion to **2Cl** is complete, this signal for the Ti(III) species (presumably $[Cp^*(tBu_3P=N)Ti^{III}]^+ [B(C_6F_5)_4]^-$) diminishes in intensity as the titanium speciation returns to mostly Ti(IV), although some Ti(III) persists in these solutions.

ortho-C–H Activation. Kinetically competitive with the above process at low pressures of H_2 is an *ortho*-C–H bond activation reaction leading to the β -haloaryl cations **3X** (Scheme 3). Compounds **3X** are likely formed via a σ -bond metathesis reaction between Ti–H and an *ortho*-C–H bond of the haloarene substrate to eliminate hydrogen, which if not removed, can render this transformation reversible. Evidence for this was provided by a measured primary kinetic isotope effect on the formation of **3Cl·THF** using the experiment outlined in Scheme 6. Cationic hydride **1** was generated in toluene by treatment of $[Cp^*(tBu_3P=N)TiCH_3]^+ [B(C_6F_5)_4]^-$ with hydrogen to give **1** as an insoluble liquid clathrate-like oil. This solution was degassed to remove hydrogen, and an excess of *ortho*-1-Cl– $C_6H_4D-d_1$ was added at low temperature. The sample was again degassed and allowed to warm, converting **1** to a mixture of isotopomers of **3Cl**, which were quenched by addition of THF; the ratio of isotopomers was determined by integration methods in the 1H and 2H NMR spectra. A 3.4:1 preponderance of **3Cl·THF-d₁** indicated a k_H/k_D of up to 3.4(2).³¹ This is slightly greater than isotope effects observed in other σ -bond metathesis reactions,^{13b} but is in line with a more linear transition state in the six-membered geometry expected for H_2 elimination from

- (22) Halogen carbon bond cleavage in aliphatic RX substrates by Ti(III): (a) Yanlong, Q.; Guisheng, L.; Huang, Y. Z. *J. Organomet. Chem.* **1990**, *381*, 29. (b) Qian, Y.; Guisheng, Z.; Xiaofan, H.; Huang, Y. Z. *Synlett* **1991**, 489. (c) Covert, K. J.; Mayol, A.-R.; Wolczanski, P. T. *Inorg. Chim. Acta* **1997**, *263*, 263. (d) Agapie, T.; Dianescu, P. L.; Mendiola, D. J.; Cummins, C. C. *Organometallics* **2002**, *21*, 1329. (e) C–O bond cleavage: Rajanbabu, T. V.; Nugent, W. A. *J. Am. Chem. Soc.* **1994**, *116*, 986.
- (23) Lagoa, A. L. C.; Diogo, H. P.; Dias, M. P.; Minas da Piedade, M. E.; Amaral, L. M. P. F.; Ribeiro da Silva, M. A. V.; Martinho Simoes, J. A.; Guedes, R. C.; Costa Cabral, B. J.; Schwarz, K.; Epple, M. *Chem.–Eur. J.* **2001**, *7*, 483 and references therein.
- (24) (a) This step may proceed with initial electron transfer to ArX, followed by C–X bond cleavage. The selectivity observed is also consistent with this path since bromobenzene is more easily reduced than chlorobenzene.^{24b} (b) Andrieux, C. P.; Blocman, C.; Dumas-Bouchiat, J.-M.; Saveant, J.-M. *J. Am. Chem. Soc.* **1979**, *101*, 3432.
- (25) (a) Alternatively, it is conceivable that $Ph\cdot$ can react with H_2 to yield benzene; this reaction is thermodynamically favorable,^{25b,c} but it is not clear that it would be kinetically significant under our conditions, especially in light of the significant quantities of biphenyl produced. (b) Mebel, A. M.; Lin, M. C.; Yu, T.; Morokuma, K. *J. Phys. Chem. A* **1997**, *101*, 3189. (c) Park, J.; Dyakov, I. V.; Lin, M. C. *J. Phys. Chem. A* **1997**, *101*, 8839.
- (26) (a) The spectra obtained do not match exactly the literature ESR spectrum of the trityl radical,^{26b} which was acquired in toluene at $-20^\circ C$. However, a spectrum of genuine trityl radical (made by dissolving the trityl radical dimer^{26c} in chlorobenzene) under our reaction conditions matched the trace we observed in solutions of $[Cp^*(tBu_3P=N)TiCH_3]^+ [B(C_6F_5)_4]^-$ generated as described. (b) Chesnut, D. B.; Sloan, G. J. *J. Chem. Phys.* **1960**, *33*, 637. (c) Volz, H.; Lotsch, W.; Schnell, H.-W. *Tetrahedron* **1970**, *26*, 5343.
- (27) Chen, E. Y.-X.; Marks, T. J. *Chem. Rev.* **2000**, *100*, 1391.
- (28) (a) Jordan, R. F.; Dasher, W. E.; Echols, S. F. *J. Am. Chem. Soc.* **1986**, *108*, 1718. (b) Jordan, R. F.; Bajgur, C. S.; Willett, R.; Scott, B. *J. Am. Chem. Soc.* **1986**, *108*, 7410. (c) Jordan, R. F.; Lapointe, R. E.; Bajgur, C. S.; Willett, R. *J. Am. Chem. Soc.* **1987**, *109*, 4111.
- (29) (a) Chase, P. A.; Piers, W. E.; Parvez, M. *Organometallics* **2000**, *19*, 2040. (b) Luinstra, G. A.; ten Cate, L. C.; Heeres, H. J.; Pattiasina, J. W.; Meetsma, A.; Teuben, J. H. *Organometallics* **1991**, *10*, 3227. (c) Pattiasina, J.; Heeres, H. J.; van Bolhuis, F.; Meetsma, A.; Teuben, J. H.; Spek, A. L. *Organometallics* **1987**, *6*, 1004.

- (30) The intensity of the ESR signal for the trityl radical, in equilibrium with its dimer, is ~ 30 times lower than the signal observed for the Ti(III) species present during the reaction.

Scheme 6



$\eta^1\text{-XC}_6\text{H}_5$ adducts.⁷ Dihydrogen elimination is thus likely preceded by rapid coordination of the haloarene to the cationic titanium center via a lone pair of electrons from the halogen to form an $\eta^1\text{-XC}_6\text{H}_5$ complex, depicted as shown in Scheme 6. Recently, excellent models for such $\eta^1\text{-XC}_6\text{H}_5$ adducts of cationic early metal compounds^{5,32} have been reported, and their formation is kinetically facile and likely not heavily influenced by the nature of X. Consistent with this is the observation that, when **1** is generated with less than 1 atm of hydrogen in the presence of an excess of $\text{C}_6\text{H}_5\text{Cl}/\text{C}_6\text{H}_5\text{Br}$ (1:1), **3Cl** and **3Br** are formed at essentially the same rate, with a final ratio of $\sim 1.0:0.7$ **3Cl:3Br** observed.³³ This observation contrasts with the above-mentioned selectivity in the direct activation of Ar-X, where the activation of bromobenzene is strongly favored over chlorobenzene. Interestingly, when the roughly 1:1 mixture of **3Cl/3Br** formed in this experiment is treated with 4 atm of H_2 (still in the presence of an excess of $\text{C}_6\text{H}_5\text{Cl}/\text{C}_6\text{H}_5\text{Br}$), the bromination **2Br** is again formed predominantly, indicating that, under these conditions, compounds **2X** are formed by hydrogenolysis of β -haloarene cations **3X** to regenerate **1**, which reacts in the Ti(III) manifold with $\text{C}_6\text{H}_5\text{X}$ as described above.

β -Halogen Elimination. Early transition metal alkyl complexes containing β -halogens are rare,³⁴ but those that are known are confined to *ortho*-haloarene complexes that are kinetically stable by virtue of the high energy benzyne intermediate produced upon transfer of the halogen to the metal.^{5,35} Nonetheless, β -halogen elimination from such compounds is thermodynamically favorable when the eliminated benzyne is trapped.

(31) Although the experiment was designed to minimize the amount of $\text{H}_2/\text{HD}/\text{D}_2$ present, its complete removal from the medium was not possible. The ratio of isotopomeric products was measured as soon as possible after conversion to **3Cl·THF** to minimize and skewing of the kinetic ratio by equilibration/scrambling involving evolved H_2/HD . The fact that the observed ratio of isotopomers did not significantly change when the measurement was performed again after 30 min is indicative that, under these conditions, conversion of the kinetic ratio of **3Cl·THF** and **3Cl·THF- d_1** to a thermodynamic mixture governed by an equilibrium isotope effect is slow under these conditions.

(32) Bouwkamp, M. W.; Budzelaar, P. H. M.; Gercama, J.; Del Hierro Morales, I.; de Wolf, J.; Meetsma, A.; Troyanov, S. I.; Teuben, J. H.; Hessen, B. J. *Am. Chem. Soc.* **2005**, *127*, 14310.

(33) (a) This observation suggests that $\text{C}_6\text{H}_5\text{Cl}$ and $\text{C}_6\text{H}_5\text{Br}$ have similar thermodynamic base strength toward **1**. Although little is known about the relative base strength of haloarenes, the fact that they are relatively weak donors suggests^{33b} that differences in donor strength to a given Lewis acid should be relatively small. Furthermore, of the halobenzene series, these two members have the most similar physical properties.^{33b} (b) Kulawiec, R. J.; Crabtree, R. H. *Coord. Chem. Rev.* **1990**, *99*, 89.

The β -halogen elimination reaction depicted in Scheme 4 was subjected to quantitative kinetic analysis by monitoring the conversion of 0.0328 M solutions of **3Cl** and **3Cl·THF** to the product **2Cl·THF** and **4Cl** via ^1H NMR spectroscopy; β -bromo elimination was studied for a 0.0328 M solution of **3Br** at 292 K. Loss of compounds **3** was observed to be first order in [**3**] over several half-lives at various temperatures in the range of 292–332 K. At 292 K, a first-order rate constant of $7.43(8) \times 10^{-5} \text{ s}^{-1}$ was observed for **3Br**, while the analogous rate for **3Cl** was not significantly different, $9.76(8) \times 10^{-5} \text{ s}^{-1}$. Eyring analysis of the rates for **3Cl** (Figure 7a) reveals a substantial enthalpic barrier of $19.7(4) \text{ kcal mol}^{-1}$ and a ΔS^\ddagger of $-10(1) \text{ eu}$, indicating that some ordering is required to achieve the four-centered transition state for β -chloro elimination.

Not surprisingly, the presence of THF hampers the elimination; k_{obs} (292 K) for **3Cl·THF** is $7.2 \times 10^{-6} \text{ s}^{-1}$.³⁶ A parallel Eyring analysis of this elimination (Figure 7b) gives a ΔH^\ddagger of $28.9(8) \text{ kcal mol}^{-1}$ and a ΔS^\ddagger of $16(1)$. That ΔS^\ddagger is now positive is suggestive of a mechanism which requires partial or complete THF dissociation prior to β -halogen elimination, as shown in Scheme 7. Addition of further equivalents of THF results in more severe rate suppression, and by assuming that base-free **3Cl** is present in a steady-state concentration in the presence of THF, an expression for k_{obs} as a function of [THF] (eq 1a) is derivable. Thus, a plot of

$$k_{\text{obs}} = \frac{k_1 k_2}{k_{-1}[\text{THF}] + k_2} \quad (1a)$$

$$\frac{1}{k_{\text{obs}}} = \frac{k_{-1}}{k_1 k_2} [\text{THF}] + \frac{1}{k_1} \quad (1b)$$

$1/k_{\text{obs}}$ versus [THF] is linear (eq 1b, Figure 7c) and allows extraction of k_1 from the y-intercept; since k_2 was measured independently in the base-free system, estimates for k_{-1} and K_{eq} for THF dissociation from **3Cl·THF** are also obtainable.

(34) (a) Stockland, R. A., Jr.; Jordan, R. F. *J. Am. Chem. Soc.* **2000**, *122*, 6315. (b) Shen, H.; Jordan, R. F. *Organometallics* **2003**, *22*, 2080. (c) Stockland, R. A., Jr.; Foley, S. R.; Jordan, R. F. *J. Am. Chem. Soc.* **2003**, *125*, 796. (d) Strazisar, S. A.; Wolczanski, P. T. *J. Am. Chem. Soc.* **2001**, *123*, 4728.

(35) (a) Kraft, B. M.; Lachicotte, R. J.; Jones, W. D. *J. Am. Chem. Soc.* **2001**, *123*, 10973. (b) van Rooyen, P. H.; Schindehutte, M.; Lotz, S. *Organometallics* **1992**, *11*, 1104.

(36) This reaction was followed only to 65% completion.

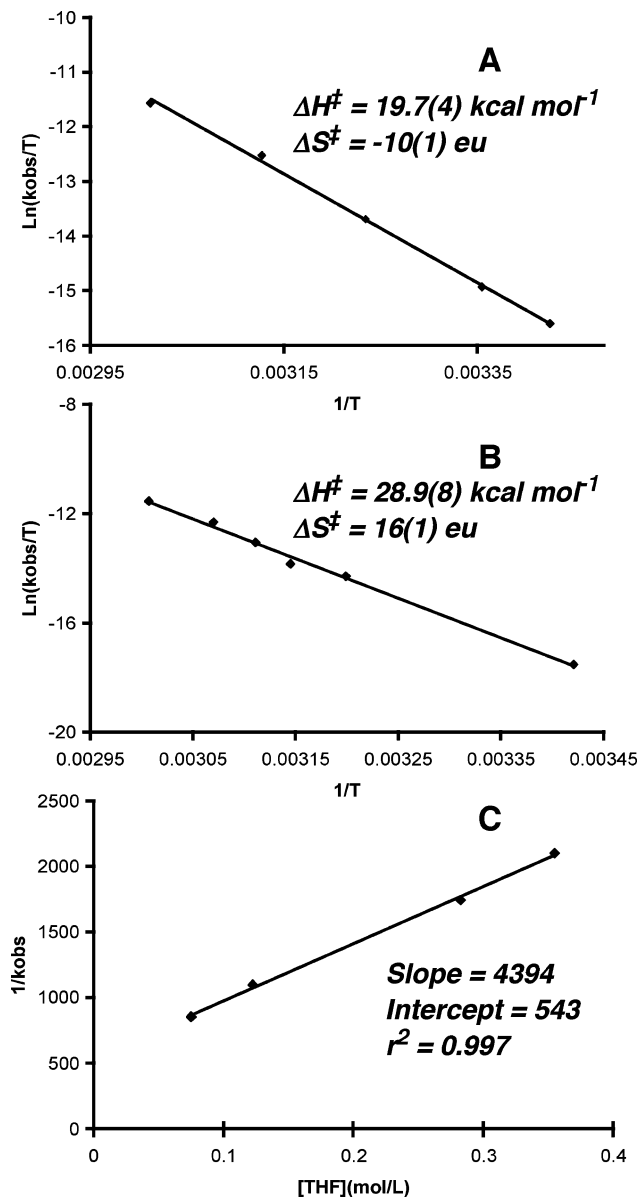
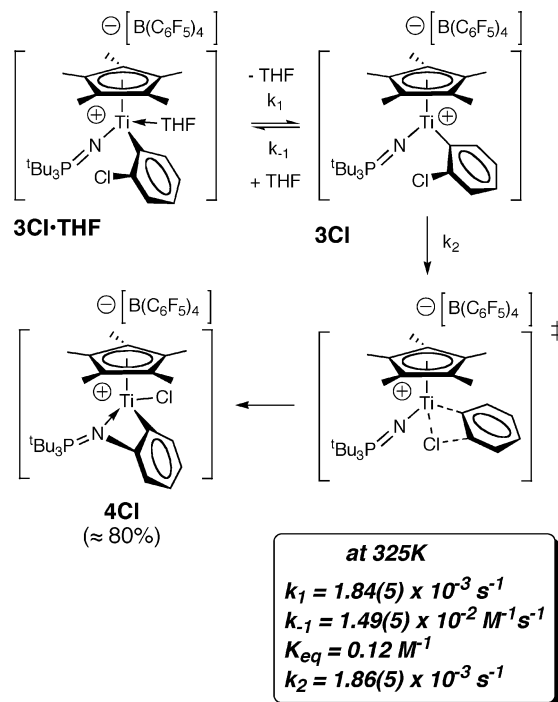


Figure 7. (a) Eyring plot of the thermolysis of **3Cl** (292–332 K) in C_6D_5Br . (b) Eyring plot of the thermolysis of **3Cl·THF** (292–332 K) in C_6D_5Br . (c) Plot of $1/k_{obs}$ versus THF concentration (0.075–0.484 M) with $[Ti] = 0.0328 \text{ M}$ for the thermolysis of **3Cl·THF**. The reactions were carried out in C_6D_5Br at 325 K. Intercept = 542.9; slope = 4349; linear correlation coefficient = 0.997.

These data are given in the legend for Scheme 7 and provide a quantitative basis for the observed rate suppression in the presence of THF. At concentrations of THF beyond the points shown in Figure 7c, rate suppression is extreme, such that the equilibrium is effectively saturated in favor of **3Cl·THF** and the rate of β -chloro elimination becomes negligible under these conditions.

Conclusions. The cationic titanium complex **1** is a rare monomeric hydrido species that while stable enough to generate and characterize is nonetheless highly reactive. This study has demonstrated its rapid reactivity with chloro- and bromobenzene by diverse pathways of bond activation, including direct C–X bond cleavage mediated by catalytic amounts of Ti(III), σ -bond metathetical elimination of H_2 for β -haloaryl cations, and β -halo elimination (indirect C–X activation) from these aryl cations.

Scheme 7



The system illustrates the range of possible pathways for the activation of such substrates by d^0 metal hydrides.

Experimental Section

General Procedures: All operations were performed under a purified argon atmosphere using glovebox or vacuum line techniques. Toluene, hexanes, and THF were dried and purified by passing through activated alumina and Q5 columns. Bromobenzene, chlorobenzene, and bromobenzene- d_5 (C_6D_5Br) were dried over CaH_2 and distilled under reduced pressure. Deuterated NMR solvents toluene- d_8 (C_7D_8) and THF- d_8 were dried and distilled from sodium/benzophenone ketyl. 1H , ^{11}B , ^{13}C , ^{19}F , and ^{31}P NMR experiments were performed on Bruker AMX-300 and DRV-400 spectrometers. Data are given in parts per million relative to residual solvent signals for 1H and ^{13}C spectra. ^{11}B , ^{19}F , and ^{31}P spectra were referenced to external $BF_3 \cdot Et_2O$, C_6H_5F , and H_3PO_4 , respectively. The ^{11}B and ^{19}F NMR spectra of the anion $[B(C_6F_5)_4]^-$ in ionic complexes do not significantly change and appear at the following positions: ^{11}B NMR (C_6D_5Br 128.2 MHz): $\delta -16.9$. ^{19}F NMR (C_6D_5Br , 282.4 MHz): $\delta -132.8$ (*ortho*-F), -163.2 (*para*-F), -167.0 (*meta*-F). Elemental analyses were performed in the microanalytical laboratory of the Department of Chemistry (University of Calgary). X-ray crystallography was performed on suitable crystals coated in paratone oil and mounted on a Rigaku AFC6S diffractometer (University of Calgary). $[Ph_3C]^+[B(C_6F_5)_4]^-$ was supplied as a generous gift by Nova Chemicals Corp. The compounds $Cp^*(Bu_3P=N)TiCl_2$, $Cp^*(Bu_3P=N)Ti(CH_3)_2$,³⁷ $[Cp^*(Bu_3P=N)TiCH_3]^+[B(C_6F_5)_4]^-$,¹⁰ and 2- 2H -chlorobenzene³⁸ were prepared by literature procedures.

Synthesis of 2Cl and 2Cl·THF. A chlorobenzene solution (0.4 mL) of $Cp^*(Bu_3P=N)Ti(CH_3)_2$ (28 mg, 0.065 mmol) was added dropwise to a chlorobenzene solution (0.4 mL) of $[Ph_3C]^+[B(C_6F_5)_4]^-$ (60 mg, 0.067 mmol) in a J-Young NMR tube at room temperature. The resulting solution was shaken for about 1 min before the NMR tube was evacuated and recharged with H_2 (ca. 4 atm). With agitation, the reaction was monitored by 1H NMR spectroscopy; when conversion

(37) Stephan, D. W.; Stewart, J. C.; Guérin, F.; Courtney, S.; Kickam, J.; Hollink, E.; Beddie, C.; Graham, T.; Wei, P.; Spence, R. E. v. H.; Xu, W.; Koch, L.; Gao, X.; Harrison, D. G. *Organometallics* **2003**, *22*, 1937.

(38) Roberts, J. D.; Simmonow, D. A.; Simmons, H. E.; Carlsmith, L. A. *J. Am. Chem. Soc.* **1956**, *78*, 601.

was complete, the volume of the reaction mixture was reduced to ca. 0.2 mL under vacuum. Hexanes (ca. 4 mL) were added, and the product was precipitated as a red solid. The supernatant was decanted, and the resulting red solid was dried under reduced pressure to afford **2Cl**. Yield, 66 mg (91%). **2Cl** was dissolved in THF to form the THF adduct **2Cl·THF** quantitatively. NMR data (C₆D₅Br) for **2Cl**: ¹H NMR δ 1.85 (s, 15H, C₅(CH₃)₅), 1.14 (d, ³J_{H-P} = 14.3 Hz, 27H, C(CH₃)₃). ¹³C NMR: δ 128.1 (C₅(CH₃)₅), 40.1 (d, ¹J_{C-P} = 40.2 Hz, PC), 29.3 (C(CH₃)₃), 13.2 (C₅(CH₃)₅). ³¹P{¹H} NMR: δ 63.2. Anal. Calcd for C₄₆H₄₂BClF₂₀NPTi: C, 49.60; H, 3.80; N, 1.26. Found: C, 49.25; H, 3.58; N, 1.58. NMR data (C₆D₅Br) for **2Cl·THF**: ¹H NMR δ 3.68 (m, 4H, OCH₂CH₂), 1.87 (s, 15H, C₅(CH₃)₅), 1.64 (m, 4H, OCH₂CH₂), 1.10 (d, ³J_{H-P} = 14.3 Hz, 27H, C(CH₃)₃). ¹³C NMR: δ 127.7 (C₅(CH₃)₅), 76.7 (OCH₂CH₂), 41.2 (d, ¹J_{C-P} = 42.3 Hz, PC), 28.9 (C(CH₃)₃), 25.6 (OCH₂CH₂), 12.2 (C₅(CH₃)₅). ³¹P{¹H} NMR (C₆D₅Br): δ 60.6. Anal. Calcd for C₅₀H₅₀BF₂₀NOPTi: C, 50.63; H, 4.25; N, 1.18. Found: C, 50.54; H, 4.60; N, 1.10.

An analogous procedure was used to produce **2Br** and **2Br·THF** in 88% yield. NMR data (C₆D₅Br) for **2Br**: ¹H NMR δ 1.87 (s, 15H, C₅(CH₃)₅), 1.17 (d, ³J_{H-P} = 14.2 Hz, 27H, C(CH₃)₃). ¹³C NMR: δ 127.8 (C₅(CH₃)₅), 42.1 (d, ¹J_{C-P} = 40.2 Hz, PC), 29.1 (C(CH₃)₃), 13.3 (C₅(CH₃)₅). ³¹P{¹H} NMR: δ 64.4. Anal. Calcd for C₄₆H₄₂BF₂₀NPBrTi: C, 47.70; H, 3.65; N, 1.21. Found: C, 48.15; H, 3.76; N, 1.27. NMR data (C₆D₅Br) for **2Br·THF**: ¹H NMR δ 3.70 (m, 4H, CH₂O), 2.18 (s, 15H, C₅(CH₃)₅), 1.70 (m, 4H, CH₂CH₂O), 1.13 (d, ³J_{H-P} = 14.0 Hz, 27H, C(CH₃)₃). ¹³C NMR: δ 129.7 (C₅(CH₃)₅), 77.3 (CH₂O), 41.4 (d, ¹J_{C-P} = 43.3 Hz, PC), 29.6 (C(CH₃)₃), 25.6 (OCH₂CH₂), 12.7 (C₅(CH₃)₅). ³¹P{¹H} NMR: δ 52.7. Anal. Calcd for C₅₀H₅₀BF₂₀NOPTi: C, 48.81; H, 4.10; N, 1.14. Found: C, 49.11; H, 3.92; N, 1.55.

Synthesis of Cp*(Bu₃P=N)Ti(CH₃)Cl. B(C₆F₅)₃ (11 mg, 0.021 mmol) was added into a toluene solution (15 mL) of Cp*(Bu₃P=N)-Ti(CH₃)₂ (192 mg, 0.45 mmol) and Cp*(Bu₃P=N)TiCl₂ (210 mg, 0.45 mmol) at room temperature. The resulting mixture was stirred overnight and a small amount oily precipitate formed. The supernatant was decanted into another flask, and its volume was reduced to 2 mL under reduced pressure. Cooling to -30 °C to afford yellow crystals. Yield, 305 mg (76%). NMR data (C₆D₆) ¹H NMR: δ 2.09 (s, 15H, C₅(CH₃)₅), 1.26 (d, ³J_{H-P} = 14.0 Hz, 27H, C(CH₃)₃), 0.92 (s, 3H, Ti-CH₃). ¹³C NMR: δ 121.4 (C₅(CH₃)₅), 47.3 (Ti-CH₃), 42.0 (d, ¹J_{C-P} = 42.1 Hz, PC), 30.4 (C(CH₃)₃), 13.0 (C₅(CH₃)₅). ³¹P{¹H} NMR: δ 37.8. Anal. Calcd for C₂₃H₄₅NPCTi: C, 61.40; H, 10.08; N, 3.11. Found: C, 61.61; H, 9.88; N, 3.35.

Generation of 2Cl from Cp*(Bu₃P=N)Ti(CH₃)Cl. A C₆D₅Br solution (0.3 mL) of Cp*(Bu₃P=N)Ti(Cl)CH₃ (24 mg, 0.053 mmol) was added dropwise to a C₆D₅Br solution (0.3 mL) of [Ph₃C]⁺[B(C₆F₅)₄]⁻ (49 mg, 0.053 mmol) in a NMR tube at room temperature. The resulting solution was shaken for about 5 min before the NMR spectra were recorded. The spectra were identical to those described above.

Determination of Organic Byproducts in Generation of 3Br. **3Br** was prepared as described above in C₆H₅Br. The reaction mixture was passed rapidly through a short silica column, followed by a small portion of pure solvent. The filtrate was analyzed by GCMS, using naphthalene as an internal standard. Products were identified by spiking with authentic samples. Ratios were determined by integration of the peak areas in the GC trace.

Synthesis of 3Cl and 3Cl·THF. Method 1: A chlorobenzene solution (2 mL) of Cp*(Bu₃P=N)Ti(CH₃)₂ (98 mg, 0.23 mmol) was added dropwise to a chlorobenzene solution (3 mL) of [Ph₃C]⁺[B(C₆F₅)₄]⁻ (210 mg, 0.23 mmol) in a 15 mL flask equipped with a Kontes valve at room temperature. The resulting solution was stirred before the headspace was evacuated and recharged with H₂ (<1 atm). The color of the reaction mixture changed rapidly from orange to red whereupon the hydrogen pressure was relieved under vacuum. Hexanes (ca. 10 mL) were condensed into the vessel, precipitating the red product. The mixture was cooled to -30 °C overnight to complete product

precipitation and the solid isolated by decanting the supernatant and washing with cold hexanes (2 mL). The solid was dried under reduced pressure to afford **3Cl**. Yield, 232 mg (85%). The compound **3Cl** was dissolved in THF to form quantitatively the THF adduct **3Cl·THF**. The X-ray quality crystals of **3Cl·THF** were grown from layering the THF solution of compound with hexane at -30 °C. Method 2: Excess chlorobenzene (5 equiv) was added into a toluene solution of [Cp*(Bu₃P=N)TiH]⁺[B(C₆F₅)₄]⁻ which was generated quantitatively by reacting [Cp*(Bu₃P=N)TiCH₃]⁺[B(C₆F₅)₄]⁻ and H₂ (4 atm) at room temperature. Upon addition, the color of the reaction mixture was changed from orange to red immediately. The volatiles were removed, and the resulting red oil was triturated with cold hexanes (3 × 2 mL) to afford **3Cl**, which was dried in vacuo. NMR data (C₆D₅-Br) for **3Cl**: ¹H NMR (263 K) δ 7.23 (d, J = 7.2 Hz, 1H, C_{aryl}H), 7.09 (d, J = 6.4 Hz, 1H, C_{aryl}H), 7.04 (t, J = 6.4 Hz, 1H, C_{aryl}H), 6.90 (t, J = 7.2 Hz, 1H, C_{aryl}H), 1.71 (s, 15H, C₅(CH₃)₅), 0.89 (d, ³J_{H-P} = 13.4 Hz, 27H, C(CH₃)₃). ¹³C NMR (263 K): δ 183.4 (Ti-C), 135.3, 130.2, 129.4 (C_{aryl}), 128.5 (C₅(CH₃)₅), 125.2, 123.1 (C_{aryl}), 40.8 (d, ¹J_{C-P} = 44.6 Hz, PC), 25.29 (C(CH₃)₃), 11.9 (C₅(CH₃)₅). ³¹P{¹H} NMR (263 K): δ 57.9. Anal. Calcd for C₅₂H₄₆BClF₂₀NPTi: C, 52.48; H, 3.90; N, 1.18. Found: C, 52.31; H, 4.35; N, 1.56. NMR data (THF-d₈) for **3Cl·THF**: ¹H NMR δ 7.45 (dd, J = 7.2 Hz, J = 2.0 Hz, 1H, C_{aryl}H), 7.30 (dd, J = 7.4 Hz, J = 1.3 Hz, 1H, C_{aryl}H), 7.11 (dt, J = 7.2 Hz, J = 2.0 Hz, 1H, C_{aryl}H), 7.01 (dt, J = 7.4, J = 1.3 Hz, 1H, C_{aryl}H), 3.64 (m, 4H, OCH₂CH₂), 2.10 (s, 15H, C₅(CH₃)₅), 1.79 (m, 4H, OCH₂CH₂), 1.57 (d, ³J_{H-P} = 13.6 Hz, 27H, C(CH₃)₃). ¹³C NMR: δ 189.3 (Ti-C), 139.5, 130.7 (C_{aryl}), 129.7 (C₅(CH₃)₅), 129.3, 129.2, 124.6 (C_{aryl}H), 68.2 (OCH₂-CH₂), 42.4 (d, ¹J_{C-P} = 42.3 Hz, PC), 30.0 (C(CH₃)₃), 26.4 (OCH₂CH₂), 13.4 (C₅(CH₃)₅). ³¹P{¹H} NMR (C₆D₅Br): δ 56.7. Anal. Calcd for C₅₆H₅₄BF₂₀NOPTi·C₄H₈O: C, 54.01; H, 4.68; N, 1.05. Found: C, 54.68; H, 4.36; N, 1.24.

Synthesis of 3Br and 3Br·THF. Analogous procedures to those described for **3Cl** and **3Cl·THF** were employed to prepare **3Br** in 88% yield. NMR data (C₆D₅Br) for **3Br**: ¹H NMR (260 K) δ 7.32 (d, J = 7.3 Hz, 1H, C_{aryl}H), 7.05 (d, J = 6.4 Hz, 1H, C_{aryl}H), 6.95 (m, 2H, C_{aryl}H), 1.76 (s, 15H, C₅(CH₃)₅), 0.96 (d, ³J_{H-P} = 13.7 Hz, 27H, C(CH₃)₃). ¹³C NMR (260 K): δ 185.0 (Ti-C), 135.2 (C_{aryl}), 129.4 (C₅(CH₃)₅), 128.7, 127.9, 125.7, 119.1 (C_{aryl}), 41.0 (d, ¹J_{C-P} = 40.6 Hz, PC), 28.5 (C(CH₃)₃), 12.3 (C₅(CH₃)₅). ³¹P{¹H} NMR (260 K): δ 57.3. Anal. Calcd for C₅₂H₄₆BBF₂₀NPTi: C, 50.59; H, 3.76; N, 1.13. Found: C, 49.96; H, 3.76; N, 1.22. NMR data (THF-d₈) for **3Br·THF**: ¹H NMR δ 7.48 (dd, J = 7.3 Hz, J = 1.9 Hz, 1H, C_{aryl}H), 7.38 (dd, J = 6.9 Hz, J = 2.4 Hz, 1H, C_{aryl}H), 7.00 (m, 2H, C_{aryl}H), 3.61 (m, 4H, OCH₂CH₂), 2.12 (s, 15H, C₅(CH₃)₅), 1.77 (m, 4H, OCH₂CH₂), 1.52 (d, ³J_{H-P} = 13.6 Hz, 27H, C(CH₃)₃). ¹³C NMR: δ 189.5 (Ti-C), 132.5, 130.8, 129.9 (C_{aryl}), 129.8 (C₅(CH₃)₅), 129.4, 124.8 (C_{aryl}), 68.4 (OCH₂CH₂), 42.6 (d, ¹J_{C-P} = 42.7 Hz, PC), 30.2 (C(CH₃)₃), 26.4 (OCH₂CH₂), 13.6 (C₅(CH₃)₅). ³¹P{¹H} NMR: δ 56.1. Anal. Calcd for C₅₆H₅₄BF₂₀NOPTi·C₄H₈O: C, 52.27; H, 4.53; N, 1.02. Found: C, 53.21; H, 4.50; N, 1.48.

Determination of the Primary Kinetic Isotope Effect in the Formation of 3Cl. [(Cp*)Ti(NP₃Bu₃H)]⁺[B(C₆F₅)₄]⁻ was generated by reacting [Cp*(Bu₃P=N)TiCH₃]⁺[B(C₆F₅)₄]⁻ and H₂ (4 atm) at room temperature in a J-Young NMR tube in toluene-d₈. Excess dihydrogen was removed, and an excess of 2-D-ClC₆H₄ was added. The NMR tubes were thoroughly shaken, and residual H₂ was removed under vacuum. THF was condensed into the NMR tube either immediately or after ~6 min at room temperature. The ¹H NMR spectra were recorded, and the ratio of isotopomers was determined by integration.

Competition Experiments. Formation of 2Cl/2Br: In a typical experiment, the compound [Cp*(Bu₃P=N)TiCH₃]⁺[B(C₆F₅)₄]⁻ was generated in a J-Young NMR tube in a mixed solvent (C₆H₅Cl:C₆H₅-Br = 1.9:1.0 or 9.4:1.0). Dihydrogen (4 atm) was admitted into the tube and the product mixture assayed by ³¹P NMR spectroscopy. The ratio of **2Cl** and **2Br** was determined by integration, and the selectivity was determined by correcting for the solvent ratio. **Formation of 3Cl/**

3Br: A method analogous to method 1 for the preparation of **3X** described above was employed using solvent mixtures of either $C_6H_5Br:C_6H_5Cl = 1:1.1$ or $C_6H_5Br:C_6H_5Cl = 1:4$. The ratio of products was determined by integration of ^{31}P NMR spectra and corrected for the solvent ratio used.

Synthesis of 4Cl. A chlorobenzene solution (1 mL) of **3Cl** (43 mg, 0.036 mmol) was stirred at room temperature for 3 days, and the color gradually turned dark. Three milliliters of hexanes was added, and the resulting solution was cooled to -30 °C to afford brown crystals of **4Cl**. Yield, 22 mg (51%). NMR data (C_6D_5Br) for **4Cl**: 1H NMR δ 7.47 (d, $J = 7.3$ Hz, 1H, $C_{aryl}H$), 7.32 (d, $J = 8.1$ Hz, 1H, $C_{aryl}H$), 7.14 (t, $J = 8.1$ Hz, 1H, $C_{aryl}H$), 6.77 (t, $J = 7.3$ Hz, 1H, $C_{aryl}H$), 1.66 (s, 15H, $C_5(CH_3)_5$), 1.11 (d, $^3J_{H-P} = 13.2$ Hz, 27H, $C(CH_3)_3$). ^{13}C NMR: δ 196.6 (Ti–C), 132.8, 132.3, 130.3 (C_{aryl}), 129.5 ($C_5(CH_3)_5$), 124.3(br), 122.7 ($C_{aryl}H$), 42.3 (br, PC), 30.1 ($C(CH_3)_3$), 12.8 ($C_5(CH_3)_5$). $^{31}P\{^1H\}$ NMR: δ 81.9. Anal. Calcd for $C_{52}H_{46}BClF_{20}NPTi$: C, 52.48; H, 3.90; N, 1.18. Found: C, 52.33; H, 3.74; N, 1.01.

Synthesis of 4Br. This compound was prepared similarly to **4Cl** in 55% yield. NMR data (C_6D_5Br) for **4Br**: 1H NMR δ 7.49 (d, $J = 7.2$ Hz, 1H, $C_{aryl}H$), 7.34 (d, $J = 7.9$ Hz, 1H, $C_{aryl}H$), 7.02 (t, $J = 7.9$ Hz, 1H, $C_{aryl}H$), 6.76 (t, $J = 7.2$ Hz, 1H, $C_{aryl}H$), 1.68 (s, 15H, $C_5(CH_3)_5$), 1.22 (d, $^3J_{H-P} = 13.2$ Hz, 27H, $C(CH_3)_3$). ^{13}C NMR: δ 199.2 (Ti–C), 132.4, 130.3 (C_{aryl}), 128.2 ($C_5(CH_3)_5$), 128.1, 124.3(br), 122.7 ($C_{aryl}H$), 41.9 (d, $J = 42.7$ Hz, PC), 29.1 ($C(CH_3)_3$), 13.3 ($C_5(CH_3)_5$). $^{31}P\{^1H\}$ NMR: δ 81.0. Anal. Calcd for $C_{52}H_{46}BBBrF_{20}NPTi$: C, 50.59; H, 3.76; N, 1.13. Found: C, 49.92; H, 3.76; N, 0.99.

Kinetic Studies of β -Halo Elimination Reactions. Stock solutions (0.0328 M) of **3Cl·THF** were prepared by dissolving 153 mg of the compound, freshly crystallized from THF in 3.5 mL of C_6D_5Br and storing frozen at -35 °C. In the glovebox, portions (0.5 mL) were

transferred into a J-Young NMR tube and kept at -78 °C prior to analysis. Solutions of **3Cl** (136 mg) and **3Br** (142 mg) were prepared similarly. Samples were warmed in a water bath prior to being introduced into a thermostated NMR probe at temperatures calibrated externally using an ethylene glycol or methanol standard. After equilibration, the reactions were monitored over time, acquiring spectra with suitable relaxation delays between pulses. For the THF-dependent studies, additional equivalents of THF were added by syringe into the NMR tubes in the glovebox in C_6D_5Br , and the concentrations of THF in the solution were calculated from the integrations of the 1H NMR signals of THF with respect to those of **3Cl·THF**, thereby taking into account the additional equivalent of free THF present in the crystalline samples of the adduct. The progress of reactions was monitored by integration of the Cp^* peak in 1H NMR spectrum. The reactions were followed for a period of at least 3 half-lives except the run for **3Cl·THF** at 292 K, which was stopped after 35 h (~65% conversion).

Acknowledgment. Funding for this work was provided by Nova Chemicals Inc. of Calgary, Alberta, and NSERC of Canada through a CRD grant to W.E.P. Mr. Edwin van der Eide is thanked for help with acquiring and interpreting the ESR spectra reported herein.

Supporting Information Available: ORTEP diagrams for the structurally characterized compounds (**3Cl·THF**, **3Br·THF**, **4Cl**, 4 pages, print/PDF). This material is available free of charge via the Internet at <http://pubs.acs.org>.

JA0583618